International Journal of Obesity (2014) **38,** 1044–1052

www.nature.com/ijo

OPEN

ORIGINAL ARTICLE

The small molecule indirubin-3′-oxime activates Wnt/β-catenin signaling and inhibits adipocyte differentiation and obesity

OM Choi[1,2], Y-H Cho[1,2], S Choi[3], S-H Lee[1,2], SH Seo[1,2], H-Y Kim[1,2], G Han[1,2], DS Min[2,4], T Park[3] and KY Choi[1,2]

OBJECTIVES: Activation of the Wnt/β-catenin signaling pathway inhibits adipogenesis by maintaining preadipocytes in an undifferentiated state. We investigated the effect of indirubin-3′-oxime (I3O), which was screened as an activator of the Wnt/β-catenin signaling, on inhibiting the preadipocyte differentiation *in vitro* and *in vivo*.
METHODS: 3T3L1 preadipocytes were differentiated with 0, 4 or 20 μM of I3O. The I3O effect on adipocyte differentiation was observed by Oil-red-O staining. Activation of Wnt/β-catenin signaling in I3O-treated 3T3L1 cells was shown using immunocytochemical and immunoblotting analyses for β-catenin. The regulation of adipogenic markers was analyzed via real-time reverse transcription-PCR (RT-PCR) and immunoblotting analyses. For the *in vivo* study, mice were divided into five different dietary groups: chow diet, high-fat diet (HFD), HFD supplemented with I3O at 5, 25 and 100 mg kg^{-1}. After 8 weeks, adipose and liver tissues were excised from the mice and subject to morphometry, real-time RT-PCR, immunoblotting and histological or immunohistochemical analyses. In addition, adipokine and insulin concentrations in serum of the mice were accessed by enzyme-linked immunosorbent assay.
RESULTS: Using a cell-based approach to screen a library of pharmacologically active small molecules, we identified I3O as a Wnt/β-catenin pathway activator. I3O inhibited the differentiation of 3T3-L1 cells into mature adipocytes and decreased the expression of adipocyte markers, CCAAT/enhancer-binding protein α and peroxisome proliferator-activated receptor γ, at both mRNA and protein levels. *In vivo*, I3O inhibited the development of obesity in HFD-fed mice by attenuating HFD-induced body weight gain and visceral fat accumulation without showing any significant toxicity. Factors associated with metabolic disorders such as hyperlipidemia and hyperglycemia were also improved by treatment of I3O.
CONCLUSION: Activation of the Wnt/β-catenin signaling pathway can be used as a therapeutic strategy for the treatment of obesity and metabolic syndrome and implicates I3O as a candidate anti-obesity agent.

International Journal of Obesity (2014) **38,** 1044–1052; doi:10.1038/ijo.2013.209

Keywords: anti-obesity drug; high-fat diet; Wnt/β-catenin pathway; indirubin-3′-oxime

INTRODUCTION

The study of adipocytes has become increasingly important due to the escalating incidence of obesity and its associated disorders. Adipocytes have a fundamental role in regulating whole-body metabolic homeostasis by storing and releasing fuel-based on energy demands. However, excess storage of energy causes obesity, type 2 diabetes, metabolic diseases and atherosclerosis.[1,2] There have been recent efforts to suppress obesity through pharmacological treatment; however, these treatments have had limited efficacy and serious side effects.[3] Therefore, a major need in the treatment of obesity is to identify for a safe therapeutic agent that reduces adipose tissue and inhibits obesity on a long-term basis.[4] Recent studies have assigned particular importance to the activated Wnt/β-catenin pathway because of its role in inhibiting adipogenesis.[5,6] The first study linking Wnt signaling to adipogenesis revealed that the ectopic expression of Wnt10b inhibited adipocyte differentiation by blocking the expression of the transcription factors, CCAAT/enhancer-binding protein α (C/EBPα) and peroxisome proliferator activated receptor γ (PPARγ).[7]

The Wnt/β-catenin signaling pathway (often called the canonical Wnt pathway) has important roles in development and tissue homeostasis, and also regulates cell proliferation and differentiation.[8] β-catenin is a major factor in the canonical Wnt pathway because the status of the pathway is determined by the activation status of β-catenin.[9,10] Activation of the Wnt/β-catenin pathway leads to increased levels of β-catenin and a concomitant decrement of PPARγ and C/EBPα, transcription factors that activate the expression of adipocyte genes. The Wnt signaling pathway may therefore be an attractive target for the development of anti-obesity drugs;[11] however, no such drug is currently available. In light of this, we used a systematic cell-based screening approach to identify small-molecule activators of the Wnt/β-catenin pathway and examined their anti-adipogenic effects. From a chemical library of pharmacologically active compounds, we selected indirubin-3′-oxime (I3O), a synthesized analog of indirubin, as a model compound to characterize the effects of activating the Wnt/β-catenin pathway with respect to inhibiting adipogenesis *in vitro* and obesity *in vivo*.

Indirubin, which is extracted from the Indigo plant (isatis root or leaf), is the main active ingredient in Danggui Longhui Wan, a Chinese medicine used for the treatment of leukemia. Synthetic indirubin analogs have exhibited antitumor activity with minor toxicity in animal models.[12,13] Sub-acute toxicity tests in rats and dogs showed that orally administered indirubin did not exhibit

[1]Department of Biotechnology, College of Life Science and Biotechnology, Yonsei University, Seoul, Korea; [2]Translational Research Center for Protein Function Control, College of Life Science and Biotechnology, Yonsei University, Seoul, Korea; [3]Department of Food and Nutrition, Yonsei University, Seoul, Korea and [4]Department of Molecular Biology, College of Natural Science, Pusan National University, Pusan, Korea. Correspondence: Dr KY Choi, Department of Biotechnology, College of Life Science and Biotechnology, Yonsei University, 134 Shinchon-Dong, Seodemun-Gu, Seoul 120-749, Korea.
E-mail: kychoi@yonsei.ac.kr
Received 30 May 2013; revised 10 October 2013; accepted 4 November 2013; accepted article preview online 15 November 2013; advance online publication, 10 December 2013

significant toxicity to organs, decrease the number of leukocytes or interfere with liver and renal functions.[14] Although I3O has already been established as a glycogen synthase kinase 3β (GSK3β) and a cyclin-dependent kinase (CDK) inhibitor with antitumor activities, its anti-adipogenic effects have not been described.[15,16] In this study, we show that I3O may be an effective yet safe therapeutic agent to inhibit adipogenesis in 3T3-L1 preadipocytes, and may prevent obesity and metabolic syndrome *in vivo* by activating the Wnt/β-catenin pathway. Thus, I3O potentially represents a new class of anti-obesity drugs.

MATERIALS AND METHODS

Reagents

The LOPAC Chemical library, Oil-red-O (ORO) powder, dexamethasone and methylisobutylxanthine were purchased from Sigma-Aldrich (St Louis, MO, USA). Insulin was purchased from Roche (San Francisco, CA, USA). I3O was purchased from Cayman Chemical (Ann Arbor, MI, USA). The C/EBPα and p-GSK3β antibodies were obtained from Cell Signaling Biotechnology (Beverly, MA, USA); the PPARγ antibody was from Abcam (Cambridge, UK); the sterol regulatory element-binding protein-1 (SREBP-1) antibody was from Santa Cruz Biotechnology (Santa Cruz, CA); the α-tubulin antibody was from Calbiochem (La Jolla, CA, USA).

Cell culture

3T3-L1 preadipocytes were provided by Dr Jaewoo Kim (Yonsei University, Seoul, Korea). 3T3-L1 cells were seeded in six-well plates at a density of 3×10^4 cells per well. The cells were grown in Dulbecco's modified Eagle medium (DMEM) with 10% calf serum (CS; Gibco, Grand Island, NY, USA) until confluent. After confluence, cells were induced to differentiate in DMEM containing 10% fetal bovine serum (FBS) and MDI (520 μM methylisobutylxanthine, 1 μM dexamethasone and 167 nM insulin) with or without I3O, valproic acid (VPA), lithium chloride (LiCl) or SB-415286. After 2 days, the medium was replaced with DMEM containing 10% FBS and 1 μg ml^{-1} insulin with or without I3O, VPA, LiCl or SB-415286. On day 4, the medium was replaced with DMEM containing 10% FBS without I3O or LiCl, and changed with fresh identical medium every 2 days upto day 14 post-induction. LiCl (20 mM) or VPA (500 mM) was used as a positive control. Undifferentiated control groups were maintained in DMEM supplemented with 10% CS, 100 units/ml penicillin and 100 μg/ml streptomycin. Cells were incubated at 37 °C in a 5% CO_2 environment.

Luciferase reporter assay

HEK293-TOP cells were seeded in 96-well plates at a density of 2.5×10^4 cells per well. Cells were treated with individual chemicals at a concentration of 20 μM for 24 h. Total cell lysates were extracted with 25 μl of 5 × Reporter Lysis Buffer per well according to the manufacturer's instruction (Promega, Madison, WI, USA). Luciferin (25 μl) was added and luciferase activity was measured using FLUOSTAR (BMG Labtech, Offenburg, Germany).

Cell viability assay

For HEK293-TOP cells, the cells were seeded in 96-well plates at a density of 2.5×10^4 cells per well and treated with the respective chemicals at a concentration of 20 μM for 24 h. For 3T3L-1 cells, the cells were seeded in six-well plates at a density of 0.5×10^5 cells per well and treated with 4 or 20 μM I3O for 4 days in undifferentiation or differentiation condition as described in 'Cell culture' section. After then, 50 μl (for HEK293-TOP cells) or 1 ml (for 3T3L-1 cells) Cell Titer (Promega) reagent was added to each well and incubated for 10 min at room temperature (RT). The intensities of luminescence were measured using FLUOSTAR.

Immunocytochemistry

Cells were fixed in 4% paraformaldehyde in phosphate-buffered saline (PBS; Gibco) for 15 min at RT, washed with PBS and permeabilized with 0.1% Triton X-100 for 15 min. The cells were blocked with 5% bovine serum albumin (BSA) and 1% goat serum in PBS for 30 min at RT and incubated with mouse anti-β-catenin antibody (BD Transduction Laboratory, Lexington, KY, USA) at a 1:100 dilution overnight at 4 °C. The cells were rinsed with PBS, incubated with Alexa Fluor 488-conjugated goat anti-mouse antibody at a 1:400 dilution for 1 h at RT and counterstained with 4′,6-diamidino-2-phenylindole (DAPI, Boehringer Mannheim, Mannheim, Germany) at a 1:5000 dilution. Images were recorded using a LSM510 META confocal microscope (Carl Zeiss, Gottingen, Germany).

ORO staining

3T3-L1 preadipocytes were seeded in a six-well plate at a density of 3×10^4 cells per well. After reaching confluence, the cells were induced to differentiate with or without I3O or LiCl as described in the 'Cell culture' section. At 14 days post differentiation, the plates were washed with PBS and stained with ORO overnight. In the morning each well was washed thoroughly with water and images of the ORO staining were recorded with a TE-2000U bright-field optical microscope (Nikon, Tokyo, Japan) and quantified for further statistical analysis. For quantification, the ORO was eluted by addition of 500 μl isopropanol containing 4% nonidet P-40 to each well and the absorbance was measured spectrophotometrically at 590 nm.

Triglyceride assay

3T3-L1 adipocytes were washed with PBS and harvested. Cells were scraped off on ice into 100 μl saline solution (2 M NaCl, 2 mM EDTA, 50 mM sodium phosphate, pH 7.4). Cell suspensions were homogenized by sonication and assayed for triglyceride content using a Triglyceride assay kit (Cayman Chemical, Ann Arbor, MI, USA).

Real time reverse transcription-PCR

Total RNA was prepared using TRIzol reagent according to the manufacturer's instructions (Invitrogen, Carlsbad, CA, USA). cDNA was synthesized from 2 μg total RNA using M-MLV reverse transcriptase and 10 μl 2 × iQ SYBR Green Supermix (Bio-Rad, Hercules, CA, USA). GAPDH was used as an endogenous control in the comparative cycle-threshold (C_T) method.

Immunoblot analysis

3T3-L1 cells were rinsed with ice-cold PBS and harvested by scraping in 120 μl of radio immunoprecipitation assay buffer (Millipore, Bedford, MA, USA). After 10 min of incubation, cells were centrifuged at 10 000 xg for 30 min. Protein samples were separated on an 8 to 12% sodium dodecyl sulfate-polyacrylamide gel. Immunoblotting was performed with primary antibody as indicated, followed by horseradish peroxidase-conjugated secondary antibodies as described previously.[17] Blots were developed using enhanced chemiluminescence and detected in a luminescent image analyzer (LAS-4000, Fujifilm, Tokyo, Japan).

β-catenin knockdown by siRNA transfection

3T3-L1 cells were transfected with 100 nM of β-catenin siRNA or control siRNA using the Attractene transfection reagent (Qiagen) in Opti-MEM. After 16 h, the medium was changed to DMEM supplemented with 10% CS and cells were differentiated with or without chemicals as previously described. β-catenin siRNA or control sequences. β-catenin siRNA-1 sense: AUUACAAUCCGGUUGUGAACGUCCC, β-catenin siRNA-1 anti-sense: GGGACGUUCACAACCGGAUUGUAAU,

β-cateninsiRNA-2 sense: UAAUGAAGGCGAACGGCAUUCUGGG
β-cateninsiRNA-2 anti-sense: CCCAGAAUGCCGUUCGCCUUCAUUA
Control siRNA sense: GCAUCAAGGUGAACUUCAA
Control siRNA anti-sense: UUGAAGUUCACCUUGAUGC

Animals, diets and I3O treatment

Fifty male C57BL/6N mice (5-week-old) were purchased from Orient (Gyeonggi-do, Korea). The mice were housed in a pathogen-free facility at Yonsei University (Seoul, Korea). After a 1-week acclimation period with a commercial diet and tap water, mice were weight-matched and divided into five different dietary groups ($n = 10$ each group): chow diet; high-fat diet (HFD, Supplementary Figure 5); HFD supplemented with I3O at 5, 25 and 100 mg kg^{-1}. The mice were weighed once a week for 8 weeks. Concentrations of plasma triglyceride (TG), free fatty acid (FFA), glucose and total cholesterol (TC) were measured using commercial kits (Bio-Clinical System, Gyeonggi-do, South Korea).

Hematoxylin and eosin (H&E) staining

Dissected tissues were fixed in 4% neutral paraformaldehyde and embedded in paraffin. The paraffin sections were cut at a thickness of 5 μm and subjected to the H&E staining. Adipocyte cell size was measured in seven randomly chosen microscopic areas from three independent animals using a TE-2000U bright-field optical microscope. The average adipocyte size was determined using Image J Software.

Immunohistochemistry

Paraffin-embedded tissue sections (4 μm each) were deparaffinized and rehydrated. The slides were autoclaved in 10 mM sodium citrate buffer for antigen retrieval and blocked in 5% BSA in PBS at RT for 1 h. The sections were incubated with primary antibody overnight at 4 °C followed by incubation with biotin-conjugated secondary antibodies for 1 h at RT. The sections were incubated with an Avidin–Biotin complex (Vector Laboratories, Burlingame, CA, USA) for 45 min, followed by diaminobenzidine (DAB) staining (Vector Laboratories). The DAB-stained preparations were visualized with a TE-2000U bright-field optical microscope.

Enzyme-linked immunosorbent assay (ELISA)

Total blood of mice was collected by cardiac puncture. The blood allows clotting for 30 min and then centrifuge for 10 min at 1000 *g* to obtain supernatant. The supernatant was subjected to ELISA analysis for insulin, resistin, IL-6, TNFα and leptin using Mouse Adipokine Magnetic Bead Panel 96-Well Plate Assay (Millipore) as described in the manufacturer's instruction.

Statistical analysis

Student's *t*-test (*in vitro*) and Kruskal–Wallis test (*in vivo*) were used for statistical analyses using GraphPad Prism software package (GraphPad Software, La Jolla, CA, USA) and Statistical Package for Social Sciences 21 (IBM, Armonk, NY, USA), respectively. *P*-values <0.05 were considered significant ($^{*}P<0.05$, $^{**}P<0.01$, $^{***}P<0.001$).

RESULTS

Screening and characterization of small molecular activators of the Wnt/β-catenin pathway that inhibit adipogenesis in 3T3-L1 preadipocytes

To identify small molecular activators of the Wnt/β-catenin pathway, we adopted a cell-based approach using HEK293 stable cells harboring the Wnt/β-catenin TOPflash reporter to screen a synthetic library of pharmacologically active compounds. A total of 1280 small molecules were tested at a final concentration of 20 μM and assayed for luciferase activity 24 h after treatment (Figure 1a). VPA (500 μM)[18,19] or LiCl (20 mM)[20] was used as a

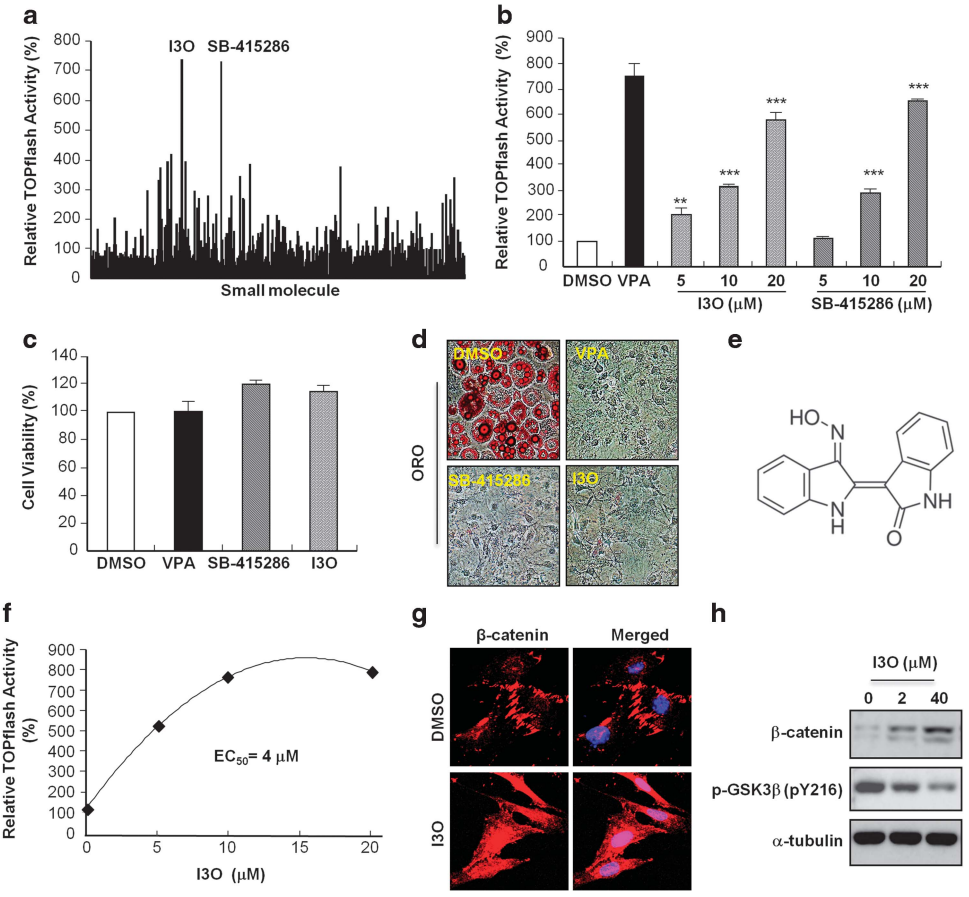

Figure 1. Screening a chemical library to identify a small molecule activator of the Wnt/β-catenin signaling pathway. (**a**) TOPflash reporter activity of HEK293-TOP cells treated with individual small molecules in DMEM at a concentration of 20 μM. After 24 h firefly luciferase activities of whole-cell lysates were measured. (**b**) Dose-dependency of I3O and SB-415286 on the activation of Wnt/β-catenin pathway in HEK293-TOP cells. VPA (500 μM) was used as a positive control (black colored bar). (**c**) Cell viability of HEK293-TOP cells was measured after treatment with either DMSO, I3O, or SB-415286 at a concentration of 20 μM. (**d**) ORO staining of 3T3-L1 preadipocytes that were induced to differentiate using MDI and treated with either DMSO, I3O or SB-415286 at a concentration of 20 μM. (**e**) Chemical structure of I3O. (**f**) Activation curve for TOPflash reporter activity induced by I3O. (**g**) 3T3-L1 preadipocytes were treated with 20 μM of I3O and immunocytochemical analysis was performed to detect β-catenin (red). Nuclei were counterstained with DAPI (blue). (**h**) 3T3-L1 preadipocytes were treated with 0, 2 and 40 μM of I3O, and immunoblotting analysis was performed to detect β-catenin, p-GSK3b (pY216) and α-tubulin. Values are mean ± standard error of the mean (s.e.m., $n=3$). $^{**}P<0.01$, $^{***}P<0.001$ (Student's *t*-test).

positive control for the activation of Wnt/β-catenin signaling. Confirmation screening identified two compounds, I3O and SB-415286, as potential candidates that activated the Wnt/β-catenin pathway; these compounds were selected for further testing (Supplementary Figure 1). Both I3O and SB-415286 dose-dependently activated TOPflash reporter activity without showing any significant cytotoxicity by the cell viability assay (Figures 1b and c). ORO staining showed that treatment with these compounds at a concentration of 20 μM markedly inhibited the adipocyte differentiation of 3T3-L1 preadipocytes without inducing abnormal cell morphologies (Figure 1d). Although both compounds showed anti-adipogenic effects, we chose I3O (Figure 1e) for further study because the anti-adipogenic effects of SB-415286 had been previously described.[21] The half-maximal effective concentration (EC_{50}) of I3O for the activation of the TOPflash reporter was 4 μM (Figure 1f). The role of I3O in the activation of the Wnt/β-catenin signaling pathway was further confirmed by the significant increase in expression and nuclear localization of β-catenin in 3T3-L1 preadipocytes (Figure 1g). The levels of β-catenin and the active form of GSK3β (p-Tyr216)[22] increased and decreased, respectively, by I3O treatment in a dose-dependent manner (Figure 1h).

I3O inhibits the differentiation of 3T3-L1 preadipocytes into adipocytes by activating the Wnt/β-catenin pathway

Treatment of differentiation-induced preadipocytes with I3O followed by ORO staining confirmed that I3O decreased the accumulation of lipid droplets in 3T3-L1 cells in a dose-dependent manner (Figure 2a). Quantitative analysis of the ORO staining showed that lipid accumulation was reduced by 38% at 4 μM and 80% at 20 μM, respectively (Figure 2b). Treatment with I3O also revealed an 82% reduction of triglyceride accumulation by 20 μM I3O (Figure 2c). The mRNA levels of both C/EBPα and PPARγ, the two major adipogenic transcription factors induced during adipocyte differentiation,[23] were significantly reduced in differentiation-induced preadipocytes treated with I3O (Figures 2d and e). mRNA levels of the PPARγ target genes, which include adipocyte protein 2 (aP2), adiponectin and lipoprotein lipase (LPL), were also significantly reduced (Supplementary Figure 2). At the protein level, the expressions of both C/EBPα and PPARγ were also reduced by I3O; concomitantly, there was an increase in β-catenin and a decrease of p-GSK3β (Figure 2f). Cell viabilities of 3T3-L1 cells were not changed by treatment of 4 μM I3O, and decreased slightly by treatment of 20 μM I3O (Supplementary Figure 3). Overall, I3O inhibits adipocyte differentiation by activating the Wnt/β-catenin pathway, resulting in the reduced expression of factors involved in adipogenesis, such as C/EBPα and PPARγ.

To confirm the involvement of the Wnt/β-catenin pathway in the anti-adipogenic effects of I3O, we measured the effects of β-catenin knockdown in MDI-induced differentiation of 3T3-L1 cells with or without I3O treatment. The β-catenin protein levels were reduced by small interference RNA (siRNA) transfection in both I3O-treated and non-treated 3T3-L1 cells (Supplementary Figure 4). ORO staining showed that the knock-down of β-catenin resulted in increased lipid accumulation compared with the control (Figures 2g and h). The induction of lipid accumulation by β-catenin knockdown was rescued by I3O. Taken together, our

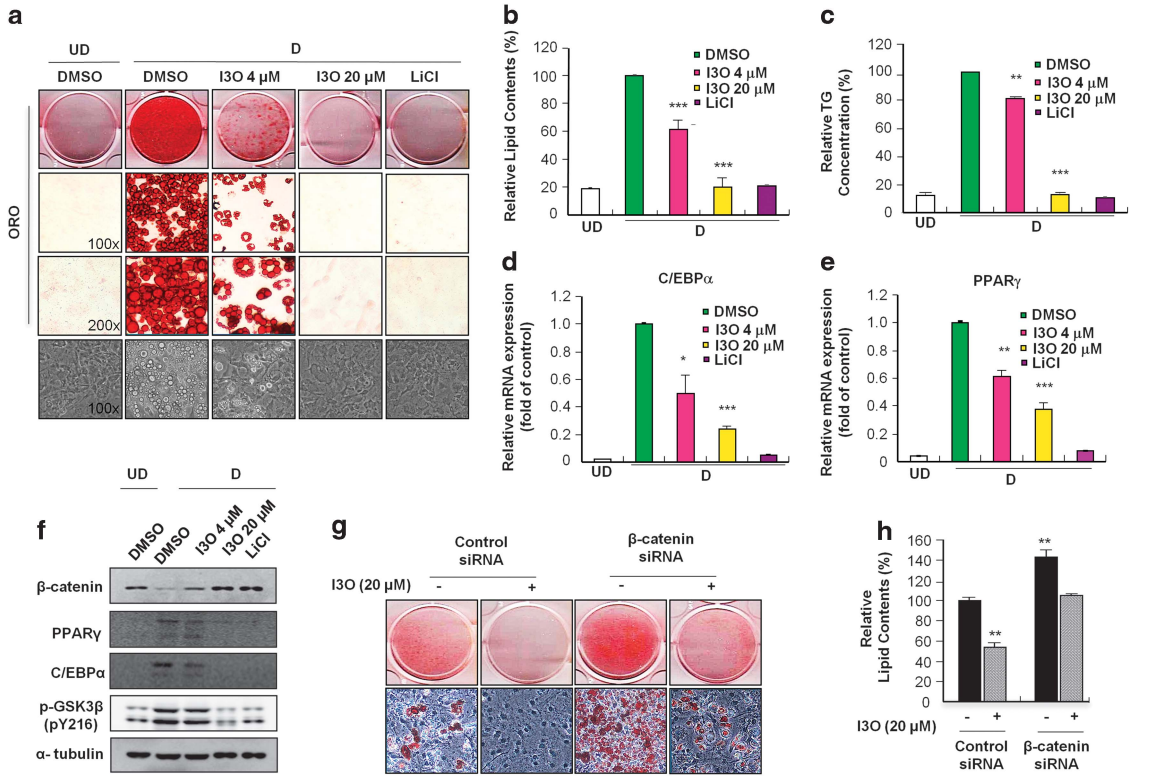

Figure 2. Effects of I3O on MDI-induced adipogenesis in 3T3-L1 cells. (**a**) 3T3-L1 preadipocytes were induced to differentiation with DMSO, 4, 20 μM I3O or 20 mM LiCl. Lipid droplets were stained using ORO 14 days post-differentiation. (**b**) ORO staining was quantified using a spectrophotometer at 590 nm. Values were normalized to the differentiated control. (**c**) 3T3-L1 preadipocytes were treated with I3O and triglyceride content was measured. Real time RT-PCR analysis of adipocyte markers PPARγ (**d**) and C/EBPα (**e**) after treatment with I3O. (**f**) Immunoblot analysis of protein expression of adipocyte markers, β-catenin, and p-GSK3β in 3T3-L1 cells that were induced to differentiation and treated with I3O. (**g**) 3T3-L1 preadipocytes were transfected with β-catenin or control siRNA. After 16 h, cells were induced to differentiate and the effects of β-catenin siRNA on the intracellular accumulation of lipid were observed by ORO staining. (**h**) Lipid accumulation was quantified using a spectrophotometer. Data are presented as mean ± s.e.m. ($n = 3$). *$P < 0.05$, **$P < 0.01$, ***$P < 0.001$ (Student's *t*-test).

data indicates that I3O inhibits adipocyte differentiation by upregulating the Wnt/β-catenin pathway.

I3O inhibits obesity in HFD-induced mice

Male C57BL/6N mice were fed a HFD supplemented with I3O (Supplementary Figure 5) for 8 weeks. Fifty mice were divided into five groups ($n = 10$ for each group): chow diet, HFD and I3O-supplemented HFD at 5, 25 and 100 mg kg^{-1} for a day. After 8 weeks, mice fed a HFD had significantly higher body weights and more abdominal fat than mice fed a chow diet (Figures 3a and b). There were no deaths or obvious signs of toxicity during the 8 weeks of feeding. Quantitative analysis of total body weight and weight gain indicated a significant reduction in obesity in the mice fed an I3O-supplemented HFD compared with mice fed a regular HFD. The average final weight of the mice was reduced by 3.3, 30 and 41% in the mice treated with 5, 25 and 100 mg kg^{-1} I3O, respectively (Figure 3b). The body weight gain was also dose-dependently reduced by treatment of I3O, with a 75% reduction in weight gain in the 100 mg kg^{-1} I3O group compared with the HFD mice (Supplementary Figure 6A). We also observed a slight reduction in daily food intake in I3O-supplemented HFD mice compared with HFD mice (Supplementary Figure 6B). To determine whether food intake had a significant role in the reduction of body weight gain, the food efficiency ratio was calculated for each group of mice (Supplementary Figure 6C). Based on the food efficiency ratio, we concluded that the food intake did not have a significant role in the reduction of body weight gain by I3O.

Visceral fat is an important indicator of metabolic syndrome and obesity.[24] To observe the effects of I3O on visceral fat, we compared the liver, epididymal, retroperitoneal, perirenal and mesenteric organs of each group of mice (Figure 3c). The visceral organs of mice treated with I3O showed a significant reduction in fat, especially in mice fed a HFD supplemented with 25 and 100 mg kg^{-1} I3O (Supplementary Figures 7A–D). Compared with the HFD mice, the total visceral fat weight was reduced by 4.8, 60 and 82% in the 5, 25 and 100 mg kg^{-1} mice, respectively (Supplementary Figure 7E).

Mice fed an I3O-supplemented HFD also showed a decrease in non-alcoholic fatty liver, a condition associated with obesity in which deposits of fat cause the liver to become enlarged and exhibit a milky pale color, showing evidence of lipid accumulation (Figure 3c). There was a significant reduction in liver weight in the I3O-supplemented HFD mice (Supplementary Figure 7F). I3O not only rescued the liver from fat accumulation and enlargement, but also from the milky pale color that results from fatty liver disease. Overall, I3O significantly prevented obesity in HFD-induced mice by decreasing visceral fat accumulation and also prevented HFD-induced fatty liver disease.

I3O improves the lipid parameters related with metabolic diseases

Two distinct phenotypes associated with metabolic diseases include hyperlipidemia and hyperglycemia.[25] To observe the

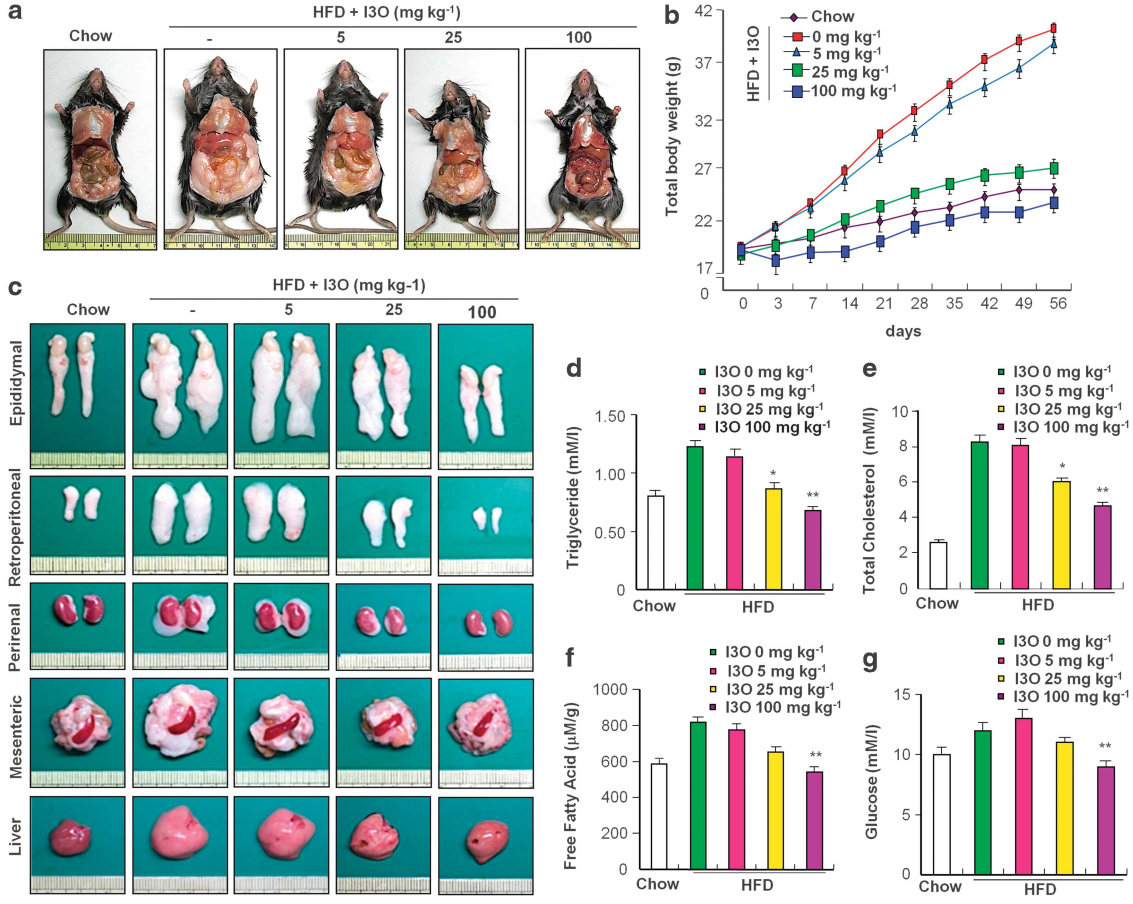

Figure 3. Effects of I3O on HFD-induced obesity in C57BL/6N mice. Fifty male C57BL/6N mice were divided into groups ($n = 10$ per group) and fed a chow diet, HFD, or HFD supplemented with I3O at 5, 25 and 100 mg kg^{-1}. (**a**) Whole-body images of Representative control and I3O-treated mice. (**b**) Total body weight. (**c**) Representative images of visceral white adipose tissue and liver of mice. Plasma levels of triglyceride (**d**), total cholesterol (**e**), free fatty acid (**f**), and glucose levels (**g**) in mice after 8 weeks of feeding with chow, HFD, or I3O-supplemented HFD. Values are expressed as means ± s.e.m. ($n = 10$). *$P < 0.05$, **$P < 0.01$, ***$P < 0.001$ (Kruskal-Wallis test).

effects of I3O on metabolic disorders, we measured plasma TG levels, TC, FFA and glucose levels in each group of mice. I3O-supplemented HFD mice showed a significant decrease in plasma TG levels compared with HFD mice: 6.7, 28.9, and 44.8% for 5, 25 and 100 mg kg^{-1} for a day, respectively (Figure 3d). There was also a dose-dependent reduction in the serum level of TC and FFA in I3O-supplemented HFD mice (Figures 3e and f). Insulin resistance is closely associated with decreased glucose uptake by muscle and fat, resulting in increased glucose levels in the blood.[26] Plasma glucose levels were significantly reduced by 13.1 and 25.6% following treatment with I3O at 25 and 100 mg kg^{-1}, respectively (Figure 3g). Overall, the reduction of plasma triglyceride and glucose levels suggests recovery from hyperlipidemia and improved cholesterol metabolism in addition to possible prevention of the onset of hyperglycemia-induced diabetes by treatment of I3O.

To further confirm the reduction of hyperlipidemia and hyperglycemia after treatment of I3O, we measured TG levels, TC and FFA levels in the liver. The liver has a vital role in fatty acid synthesis and metabolism. Fatty acid synthesized by the liver is converted to TG and transported to the blood.[27] Both TG and TC levels in the liver were significantly reduced following I3O treatment, correlating with the reduction in plasma TG and TC levels (Figures 4a and b). Lastly, FFA levels in the liver were reduced by 18.1, 44.7 and 66.6% in 5, 25 and 100 mg kg^{-1} mice, respectively (Figure 4c). Overall, I3O inhibited lipogenesis in the liver, thereby decreasing the secretion and mobilization of lipids into the bloodstream.

Next, we performed immunohistochemical analyses of β-catenin, PPARγ, C/EBPα, SREBP-1 and F4/80 expression in the liver region (Figure 4d). Consistent with *in vitro* results, mice fed a HFD showed significantly increased nuclear localization of PPARγ compared with mice fed a chow diet. However, this increase in PPARγ expression was significantly reduced in mice fed an I3O-supplemented HFD. The HFD-induced expression of SREBP-1, an adipogenic transcriptional factor,[28] was also reduced by I3O treatment. In addition, the stabilization and nuclear localization of β-catenin was significantly increased in the I3O-supplemented HFD mice compared with the HFD-induced mice. Furthermore, I3O reduced expression of the macrophage-specific marker, F4/80, indicating that I3O prevents HFD-induced infiltration of macrophages, thereby decreasing adipose tissue inflammation. In contrast to adipocytes, the expression of C/EBPα was not significantly affected in the HFD or I3O-supplemented HFD mice. C/EBPα is an abundant transcription factor in the liver, where it is involved in bilirubin detoxification and other metabolic functions.[28,29]

I3O reduces adipocyte size in white adipose tissue

The reduction of epididymal white adipose tissue in I3O-supplemented HFD mice was primarily due to significantly smaller adipocytes, as shown by 59 and 72% reductions in adipocyte size in 25 and 100 mg kg^{-1} mice, respectively (Figures 5a and b). We further confirmed the decrease in visceral white adipose tissue by examining the effect of I3O on subcutaneous fat (Figures 5c and d). The thickness of fat between the skin and muscle layers decreased significantly in the I3O-supplemented HFD mice compared with HFD mice. We confirmed the reduction in expression levels of PPARγ and C/EBPα mRNA (Figures 5e and f). Additionally, the mRNA levels of PPARγ target genes, aP2, adiponectin and LPL, were also significantly reduced (Supplementary Figures 8A–C). To monitor the glucose homeostasis, we determined the concentrations of insulin and

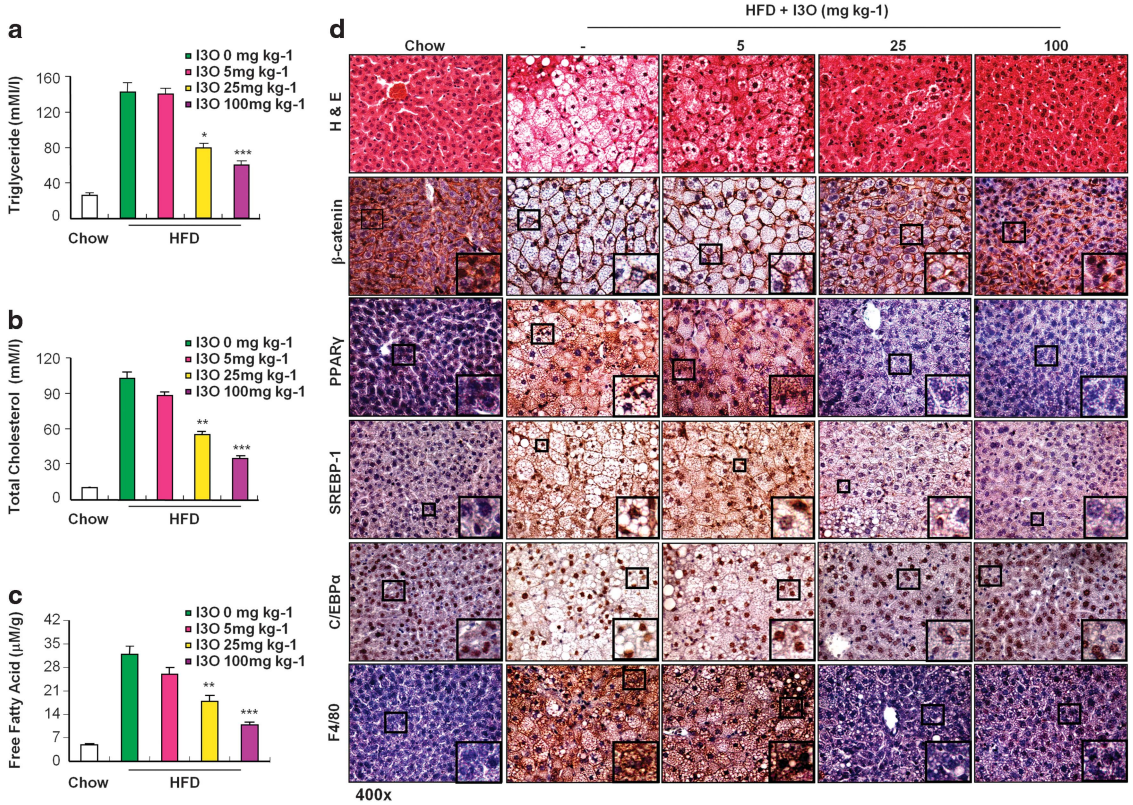

Figure 4. Effects of I3O on the liver of HFD-induced mice. Plasma levels of triglyceride (**a**), total cholesterol (**b**), and free fatty acid (**c**) in the liver of mice after 8 weeks. (**d**) Immunohistochemical analysis of markers in liver. Values are expressed as means ± s.e.m. ($n = 10$). $^{*}P < 0.05$, $^{**}P < 0.01$, $^{***}P < 0.001$ (Kruskal-Wallis test).

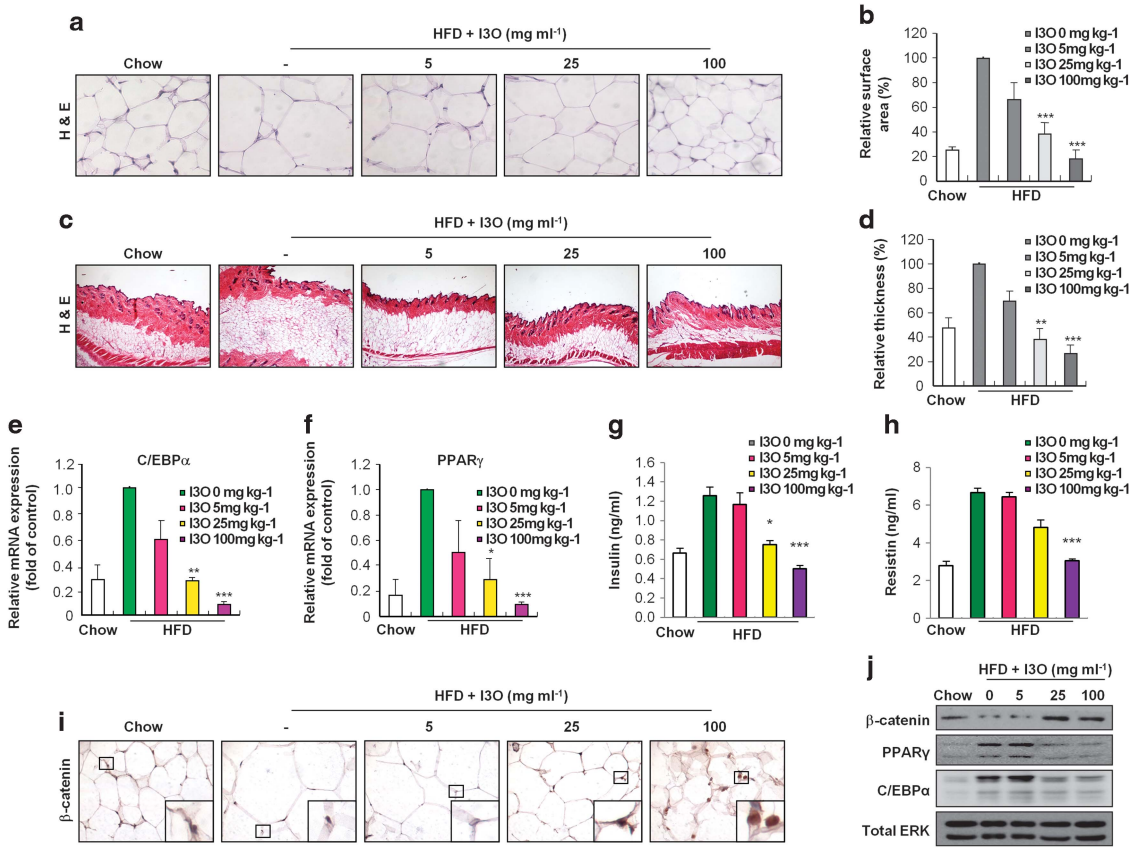

Figure 5. Effects of I3O on adipose tissue. (**a**) Histological analysis of epididymal white adipose tissue of mice fed with chow, HFD, or I3O-supplemented HFD. Tissues were stained with hematoxylin and eosin (H&E). (**b**) Adipocyte size was measured using Image J Software. (**c**) H&E staining of subcutaneous fat of mice. (**d**) Thickness of fat between skin and muscle region was measured using Image J Software. RT-PCR analysis of adipocyte markers C/EBPα (**e**) and PPARγ (**f**). Concentrations of insulin (**g**) and resistin (**h**) in the bloods of mice fed with chow, HFD, or I3O-supplemented HFD were measured using ELISA. (**i**) Immunohistochemistrical analyses were performed to detect β-catenin in epidermis fat tissues of mice fed with chow, HFD, or I3O-supplemented HFD. (**j**) Immunoblot analyses to detect expression levels of β-catenin, PPARγ, C/EBPα and ERK. Data are presented as mean ± s.e.m. ($n = 3$). *$P < 0.05$, **$P < 0.01$, ***$P < 0.001$ (Kruskal-Wallis test).

adipokines in the blood of I3O-fed and non-fed mice (Figures 5g and h and Supplementary Figures 8D–F). The higher insulin concentration in the HFD-fed mice decreased in a dose-dependent manner by the treatment of I3O (Figure 5g). Moreover, the insulin concentration in the blood of mice fed with 100 mg kg^{-1} I3O was lower than the mice fed a chow diet (Figure 5g). The concentrations of resistin, IL-6, TNFα and leptin, adipokines known to increase insulin resistance,[30] were elevated by the HFD, and in contrast, were reduced by I3O in a dose-dependent manner (Figure 5h and Supplementary Figures 8D–F). Immunohistochemical analyses for β-catenin in the epidermal fat of the I3O-fed mice showed a significant increase of nuclear β-catenin in the adipocytes (Figure 5i). We further confirmed the I3O-mediated reduction of PPARγ and C/EBPα by immunoblotting analyses (Figure 5j). Collectively, these findings verify that I3O reduces both subcutaneous and visceral fat by decreasing adipocyte size through the inhibition of PPARγ and C/EBPα via activation of Wnt/β-catenin signaling.

DISCUSSION

Given the progressive increase in the number of obese individuals in the general population, obesity has become a growing public health concern. Although diet and regular exercise may decrease the onset of obesity, these factors alone may be insufficient to combat this growing problem. There have been recent efforts to suppress obesity through pharmacological treatment; however, the currently available drugs show minimal efficacy. Many anti-obesity drugs that were initially approved by the United States Food and Drug Administration (FDA) have since been withdrawn because of serious adverse effects, especially cardiovascular-related risks.[31] For this reason, there is a pressing need to identify safer, more effective treatments to inhibit obesity on a long-term basis.[32] Currently, there are three FDA-approved anti-obesity drugs, Orlistat, Belviq and Qsymia. The latter two drugs were approved in June and July of 2012 to alleviate the unmet need for effective and safe therapies. Orlistat, a drug that blocks digestion and the absorption of fat in the intestine, and Belviq, a serotonin receptor agonist, are considered safer drugs; however, they only result in a 3–5% mean weight loss. Of these three agents, Qsymia is the most effective (9–10% mean weight loss) but increased risks of birth defects, somnolence and paraesthesia have been reported.[33] For morbidly obese patients, the weight loss associated with taking these drugs may be minimal and the side effects may outweigh the benefits.

Recent studies show that exposure to a Wnt ligand inhibits adipogenesis by blocking the differentiation of committed preadipocytes into mature adipocytes,[34,35] thus implicating small molecular activators of the Wnt/β-catenin pathway as potential therapeutic agents for obesity. In this study, we identified and characterized I3O, an indirubin analog, as a Wnt/β-catenin signaling activator with anti-obesity activity. I3O inhibited the expression of PPARγ and C/EBPα, two transcription factors that induce adipocyte gene expression.[36] The direct regulation of

adipogenesis could provide a more effective way for anti-obesity therapy than drugs targeting lipid synthesis or regulating appetite. More importantly, we also showed that I3O is a safe drug, causing no organ abnormalities and no lethality in all 30 mice that were treated with I3O for 8 weeks.

Previous studies have shown that orally administered indirubin (100–400 mg kg^{-1}) given for 30 consecutive days did not show significant toxicity to organs, decrease the number of leukocytes or interfere with liver and renal functions. Moreover, no significant abnormality was observed in dogs given indirubin (20–40 mg kg^{-1}) for up to 3 consecutive months. In clinical trials where indirubin was given orally (150–450 mg kg^{-1}), 314 patients with chronic granulocytic and myelocytic leukemia experienced either complete remission (82 cases, 26%), partial remission (105 cases, 33%) or beneficial effects (87 cases, 28%) without major side effects.[37]

Obesity is a risk factor for metabolic diseases and is often associated with co-morbidities such as diabetes.[38–40] Weight reduction is associated with the amelioration of insulin sensitivity, which intensifies the inter-relationship between obesity, diabetes and metabolic disorders. Consequently, obesity is an attractive therapeutic target for reducing the features of metabolic disorders and improving insulin resistance.[41] To further validate the effectiveness of I3O against obesity and metabolic syndrome we used a HFD-induced obesity mouse model.[42] HFD induces obesity in both humans and mice,[43] and mimics the high-fat/high-density foods that contribute to obesity in Western cultures. I3O significantly decreased body weight gain and effectively decreased total body weight in C57BL/6N mice fed a HFD. As obesity is associated with the loss of glucose homeostasis and lipid metabolism, we examined the blood constituents of mice fed with I3O-supplemented HFD. Our results indicate that I3O improves glucose and lipid metabolism without lipotoxicity. We observed a decrease in the mRNA level of adiponectin, an adipokine increasing insulin sensitivity, in adipose tissue of I3O-supplemented HFD-fed mice. However, in the blood of these mice, the adipokines increasing insulin resistance, such as resistin, IL-6, TNFα and leptin, decreased dramatically. Therefore, the overall insulin sensitivity of the mice would be improved. The HFD induced a higher insulin concentration in the blood of mice; however, the I3O-fed mice had reduced concentrations, indicating that I3O rescued HFD mice from insulinemia. Improved insulin sensitivity enhances energy consumption in the body overall; therefore, excess energy would be used up rather than being accumulated in non-fat tissues.

The direct effects of I3O on liver tissue would prevent fatty liver and improve lipid metabolism. In this study, the HFD-induced expression of adipogenic transcription factors, such as PPARγ, C/EBPα and SREBP-1, was suppressed by I3O treatment by activating Wnt/β-catenin signaling, which is known to suppress adipogenic regulation of hepatic satellite cells.[44] These results indicate that I3O suppresses adipogenesis via direct activation of Wnt/β-catenin signaling in liver tissue. In addition, the reduction of plasma and hepatic TG levels, TC and FFA levels indicate that I3O may improve lipid metabolism by acting on liver tissue. The dual effect of I3O, suppressing insulin resistant-adipokine production of fat tissues and preventing adipogenic regulations on non-fat tissues, abolishes the concern of lipotoxicity and suggests a possibility to develop an anti-obesity therapy without diet adjustments.

Lastly, we found that I3O can be administered orally as a food supplement. Thus, small molecules that activate the Wnt/β-catenin pathway represent a potential new class of anti-obesity drugs that can be easily administered. The clinical implications and significance of I3O in regulating obesity and metabolic syndrome largely reflect its ability to recover lipid metabolism and glucose homeostasis. Therefore, we propose that administration of the small molecule, I3O, may be an effective therapy to inhibit obesity and to improve the metabolic syndrome. We demonstrated the effect of I3O using a HFD-induced obesity mouse model as a representative model of human obesity.[45] However, obesity in humans is caused by various factors rather than a single environmental factor.[45] This aspect should be considered when extrapolating the mouse model studies for human application.

CONFLICT OF INTEREST

The authors declare no conflict of interest.

ACKNOWLEDGEMENTS

This work was supported by grants from the National Research Foundation (NRF) funded by the Ministry of Future Creation and Science (MFCS) of Korea through the Translational Research Center for Protein Function Control (2009-0092955), Mid-career Researcher Program National Leading Research Lab (2012-010285), Stem Cell Research Project (2010-0020235).

REFERENCES

1 Kopelman P. Obesity as a medical problem. *Nature* 2000; **404**: 635–643.
2 Lobstein T, Baur L, Uauy R. Obesity in children and young people: a crisis in public health. *Obes Rev* 2004; **5**(Suppl 1): S4–S85.
3 Cooke D, Bloom S. The obesity pipeline: current strategies in the development of anti-obesity drugs. *Nat Rev Drug Discov* 2006; **5**: 919–931.
4 Klonoff DC, Greenway F. Drugs in the pipeline for the obesity market. *J Diabetes Sci Technol* 2008; **2**: 913–918.
5 Prestwich TC, MacDougald OA. Wnt/beta-catenin signaling in adipogenesis and metabolism. *Curr Opin Cell Biol* 2007; **19**: 612–617.
6 Takada I, Kouzmenko AP, Kato S. Wnt and PPARγ signaling in osteoblastogenesis and adipogenesis. *Nat Rev Rheumatol* 2009; **5**: 442–447.
7 Ross SE, Hemati N, Longo KA, Bennett CN, Lucas PC, Erickson RL *et al.* Inhibition of adipogenesis by Wnt Signaling. *Science* 2000; **289**: 950–953.
8 Reya T, Clevers H. Wnt signaling in stem cells and cancer. *Nature* 2005; **434**: 843–850.
9 Komiya Y, Habas R. Wnt signal transduction pathways. *Organogenesis* 2008; **4**: 68–75.
10 Moon RT, Bowerman B, Boutros M, Perrimon N. The promise and perils of Wnt signaling through beta-catenin. *Science* 2002; **296**: 1644–1646.
11 Christodoulides C, Lagathu C, Sethi JK, Vidal-Puig A. Adipogenesis and WNT signalling. *Trends Endocrinol Metab* 2009; **20**: 16–24.
12 Shin EK, Kim JK. Indirubin derivative E804 inhibits angiogenesis. *BMC Cancer* 2012; **12**: 164.
13 Zhang X, Song Y, Wu Y, Dong Y, Lai L, Zhang J *et al.* Indirubin inhibits tumor growth by antitumor angiogenesis via blocking VEGFR2-mediated JAK/STAT3 signaling in endothelial cell. *Int J Cancer* 2011; **129**: 2502–2511.
14 Hoessel R, Leclerc S, Endicott JA, Nobel ME, Lawrie A, Tunnah P *et al.* Indirubin, the active constituent of a Chinese antileukaemia medicine, inhibits cyclin-dependent kinases. *Nat Cell Biol* 1999; **1**: 60–67.
15 Marko D, Schätzle S, Friedel A, Genzlinger A, Zankl H, Meijer L *et al.* Inhibition of cyclin-dependent kinase 1 (CDK1) by indirubin derivatives in human tumour cells. *Br J Cancer* 2001; **84**: 283–289.
16 Polychronopoulos P, Magiatis P, Skaltsounis AL, Myrianthopoulos V, Mikros E, Tarricone A *et al.* Structural basis for the synthesis of indirubins as potent and selective inhibitors of glycogen synthase kinase-3 and cyclin-dependent kinases. *J Med Chem* 2004; **47**: 935–946.
17 Jeong WJ, Yoon JY, Park JC, Lee SH, Lee SH, Kaduwal S *et al.* Ras stabilization through aberrant activation of Wnt/β-catenin signaling promotes intestinal tumorigenesis. *Sci Signal* 2012; **5**: r30a.
18 Gould TD, Manji HK. The Wnt signaling pathway in bipolar disorder. *Neuroscientist* 2002; **8**: 497–511.
19 Lee SH, Zahoor M, Hwang JK, Min do S, Choi KY. Valproic acid induces cutaneous wound healing *in vivo* and enhances keratinocyte motility. *PLoS One* 2012; **7**: e48791.
20 Lee SH, Kim B, Oh MJ, Yoon J, Kim HY, Lee KJ *et al.* Persicaria hydropiper (L.) Spach and its flavonoid components, isoquercitrin and isorhamnetin, activate the Wnt/β-catenin pathway and inhibit adipocyte differentiation of 3T3-L1 cells. *Phytother Res* 2011; **25**: 1629–1635.
21 Sen B, Xie Z, Case N, Ma M, Rubin C, Rubin J. Mechanical strain inhibits adipogenesis in mesenchymal stem cells by stimulating a durable beta-catenin signal. *Endocrinology* 2008; **149**: 6065–6075.

22 ter Haar E, Coll JT, Austen DA, Hsiao HM, Swenson L, Jain J. Structure of GSK3beta reveals a primed phosphorylation mechanism. *Nat Struct Biol* 2001; **8**: 593–596.
23 Després JP, Lemieux I. Abdominal obesity and metabolic syndrome. *Nature* 2006; **444**: 881–887.
24 Grundy SM. Does a diagnosis of metabolic syndrome have value in clinical practice? *Am J Clin Nutr* 2006; **83**: 1248–1251.
25 Delarue J, Magnan C. Free fatty acids and insulin resistance. *Curr Opin Cin Nutr Metab Care* 2007; **10**: 142–148.
26 Jensen-Urstad AP, Semenkovich CF. Fatty acid synthase and liver triglyceride metabolism: housekeeper or messenger? *Biochim Biophys Acta* 2012; **1821**: 747–753.
27 Horton JD, Shimomura I, Ikemoto S, Bashmakov Y, Hammer RE. Overexpression of sterol regulatory element-binding protein-1a in mouse adipose tissue produces adipocyte hypertrophy, increased fatty acid secretion, and fatty liver. *J Biol Chem* 2003; **278**: 36652–36660.
28 Darlington GJ, Wang N, Hanson RW. C/EBP alpha: a critical regulator of genes governing integrative metabolic processes. *Curr Opin Genet Dev* 1995; **5**: 565–570.
29 Lee YH, Sauer B, Johnson PF, Gonzalez FJ. Disruption of the c/ebp alpha gene in adult mouse liver. *Mol Cell Biol* 1997; **17**: 6014–6022.
30 Falcão-Pires I, Castro-Chaves P, Miranda-Silva D, Lourenço AP, Leite-Moreira AF. Physiological, pathological and potential therapeutic roles of adipokines. *Drug Discov Today* 2012; **17**: 880–889.
31 Hiatt WR, Goldfine AB, Kaul S. Cardiovascular risk assessment in the development of new drugs for obesity. *JAMA* 2012; **308**: 1099–1100.
32 Wong D, Sullivan K, Heap G. The pharmaceutical market for obesity therapies. *Nat Rev Drug Discov* 2012; **1**: 669–670.
33 Cristancho AG, Lazar MA. Forming functional fat: a growing understanding of adipocyte differentiation. *Nat Rev Mol Cell Biol* 2011; **12**: 722–734.
34 Ross SE, Erickson RL, Gerin I, DeRose PM, Bajnok L, Longo KA *et al.* Microarray analyses during adipogenesis: understanding the effects of Wnt signaling on adipogenesis and the roles of liver X receptor α in adipocyte metabolism. *Mol Cell Biol* 2002; **22**: 5989–5999.
35 Rosen ED, MacDougald OA. Adipocyte differentiation from the inside out. *Nat Rev Mol Cell Biol* 2006; **7**: 885–896.
36 Eisenbrand G, Hippe F, Jakobs S, Muehlbeyer S. Molecular mechanisms of indirubin and its derivatives: novel anticancer molecules with their origin in traditional Chinese phytomedicine. *J Cancer Res Clin Oncol* 2004; **130**: 627–635.
37 Gan WJ, Yang T, Wen S, Liu Y, Tan Z, Deng C *et al.* Studies on the mechanism of indirubin action in the treatment of chronic myelocytic leukemia (CML). II. 5′-Nucleotidase in the peripheral white blood cells of CML. *Chin Acad Med Sci Beijing* 1985; **6**: 611–613.
38 Grundy SM. What is the contribution of obesity to metabolic syndrome? *Endocinol Metab Clin North Am* 2004; **33**: 267–282.
39 Mokdad AH, Ford ES, Bowman BA, Dietz WH, Vinicor F, Bales VS *et al.* Prevalence of obesity, diabetes, and obesity-related health risk factors, 2001. *JAMA* 2003; **289**: 76–79.
40 Shafrir E. Development and consequences of insulin resistance: lessons from animals with hyperinsulinaemia. *Diabetes Metab* 1996; **22**: 122–131.
41 Fonseca VA. The metabolic syndrome, hyperlipidemia, and insulin resistance. *Clin Cornerstone* 2005; **7**: 61–72.
42 Choi Y, Kim Y, Park S, Lee KW, Park T. Indole-3′-carbinol prevents diet-induced obesity through modulation of multiple genes related to adipogenesis, thermogenesis or inflammation in the visceral adipose tissue of mice. *J Nutr Biochem* 2012; **23**: 1732–1739.
43 Hariri N, Thibault L. High-fat diet-induced obesity in animal models. *Nutr Res Rev* 2010; **23**: 270–299.
44 Cheng JH, She H, Han YP, Wang J, Xiong S, Asahina K *et al.* Wnt antagonism inhibits hepatic stellate cell activation and liver fibrosis. *Am J Physiol Gastrointest Liver Physiol* 2008; **294**: 39–49.
45 Fellmann L, Nascimento AR, Tibiriça E, Bousquet P. Murine models for pharmacological studies of the metabolic syndrome. *Pharmacol Ther* 2013; **137**: 331–340.

Supplementary Information accompanies this paper on International Journal of Obesity website (http://www.nature.com/ijo)